JOURNAL OF THE AMERICAN CHEMICAL SOCIETY

Article

pubs.acs.org/JACS

Efficient Synthesis and In Vivo Incorporation of Acridon-2-ylalanine, a Fluorescent Amino Acid for Lifetime and Förster Resonance Energy Transfer/Luminescence Resonance Energy Transfer Studies

Lee C. Speight,[†] Anand K. Muthusamy,[†] Jacob M. Goldberg,[†] John B. Warner,[†] Rebecca F. Wissner,[†] Taylor S. Willi,[‡] Bradley F. Woodman,[‡] Ryan A. Mehl,[*,‡] and E. James Petersson[*,†]

[†]University of Pennsylvania, Department of Chemistry, 231 South 34th Street, Philadelphia, Pennsylvania, 19104-6323, United States

[‡]Oregon State University, Department of Biochemistry and Biophysics, 2011 Ag Life Sciences Building, Corvallis, Oregon 97331-7305, United States

Supporting Information

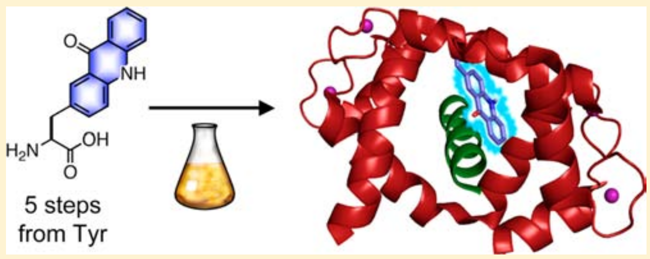

ABSTRACT: The amino acid acridon-2-ylalanine (Acd) can be a valuable probe of protein conformational change because it is a long lifetime, visible wavelength fluorophore that is small enough to be incorporated during ribosomal biosynthesis. Incorporation of Acd into proteins expressed in *Escherichia coli* requires efficient chemical synthesis to produce large quantities of the amino acid and the generation of a mutant aminoacyl tRNA synthetase that can selectively charge the amino acid onto a tRNA. Here, we report the synthesis of Acd in 87% yield over five steps from Tyr and the identification of an Acd synthetase by screening candidate enzymes previously evolved from *Methanococcus janaschii* Tyr synthetase for unnatural amino acid incorporation. Furthermore, we characterize the photophysical properties of Acd, including quenching interactions with select natural amino acids and Förster resonance energy transfer (FRET) interactions with common fluorophores such as methoxycoumarin (Mcm). Finally, we demonstrate the value of incorporation of Acd into proteins, using changes in Acd fluorescence lifetimes, Mcm/Acd FRET, or energy transfer to Eu^{3+} to monitor protein folding and binding interactions.

■ INTRODUCTION

Fluorescence spectroscopy is a powerful technique for monitoring protein folding and dynamics. Fluorescence experiments can be carried out with nanosecond time resolution, at the single molecule level, and in real time in living cells. Structural information can be derived from fluorescence experiments by exploiting distance-dependent interactions such as Förster resonance energy transfer (FRET) or fluorescence quenching through photoinduced electron transfer (PET).[1−5] Making such measurements in a time-resolved manner allows for the tracking of protein conformation as two regions of the protein undergo relative translational and rotational motion. The developments in spectroscopy over the last 25 years have afforded tremendous improvements in sensitivity as well as temporal and spatial resolution. Today, the information that one can derive from these experiments is often limited not by instrumentation but by one's ability to label the protein in an efficient, site-specific, and nonperturbing manner.

Many strategies exist for fluorescently labeling proteins, each with advantages and drawbacks. Use of the intrinsic fluorescence of Trp and Tyr is often limited to relatively small or simple proteins because most large proteins have multiple Trp or Tyr residues, complicating the interpretation of fluorescence data. The most common extrinsic labeling strategies use genetic fusions of green fluorescent protein (GFP) or its derivatives, but the large size of GFP may perturb the folding event of interest.[6−8] Smaller synthetic fluorophores can often be attached in an amino acid specific manner, for example, by exploiting the unusual reactivity of the Cys thiol.[9] However, if one wishes to carry out experiments in vivo or in cell lysate, reaction with a specific Cys is extremely difficult to achieve.

To gain greater specificity in vivo, tag sequences can be inserted in the protein, which are then modified. These tag sequences range from sizes comparable to GFP to stretches of only six amino acids.[10,11] The tag modification can be purely chemical such as the binding of arsenical fluorophore compounds (e.g., FlAsH) to a CCPGCC motif, or it can be a more complex chemoenzymatic process.[12−23] While these are valuable methods for labeling proteins, fluorescent amino acids that are incorporated cotranslationally have the potential to provide much more information on protein folding. They can be used to monitor proteins as they fold on the ribosome, and they can be placed at interior locations that are unavailable to modification after folding of the protein.[24] Several examples of incorporation of fluorescent amino acids have been demonstrated by semisynthesis of aminoacyl tRNA that is then used

Received: April 1, 2013
Published: December 4, 2013

for in vitro translation with reconstituted ribosomes or injection into *Xenopus* oocytes.[25−29] To our knowledge, only one visible-wavelength fluorescent amino acid has been shown to be compatible with site-specific in vivo incorporation in *Escherichia coli* (also two in eukaryotic cells).[30−36]

Here, we develop methods for the efficient synthesis and in vivo incorporation of acridon-2-ylalanine (**1**, Acd, δ), a blue-wavelength fluorescent amino acid. Acd is a useful fluorophore because of its small size (222 Å^3), near unity quantum yield in water (Φ = 0.95), unusually long lifetime ($\tau \sim 15$ ns) and high photostability (<5% degradation after 3 h irradiation).[37−39] Previous work in the Petersson laboratory has shown that Acd can be efficiently quenched by a thioamide through a PET mechanism.[37] This makes the Acd/thioamide pair an extremely small, nonperturbing set of labels since Acd is only 47% larger than Trp, and the thioamide is essentially isosteric with an amide. In addition, Acd can also act as a FRET partner with appropriately matched fluorophores, and Acd can be used to sensitize Eu^{3+} emission via a luminescence resonance energy transfer (LRET) mechanism.[40,41]

Sisido and co-workers have previously shown that Acd can be ribosomally incorporated into proteins by in vitro translation using the PURE system.[38] However, protein yields from systems using semisynthetic tRNA are inherently limited because the aminoacyl tRNA is rapidly hydrolyzed in the translation mixture. Also, in vitro translation on the scale necessary to produce milligrams of protein for biochemical studies is not often practiced and may require specialized expertise.[42,43] On the other hand, the in vivo incorporation methods pioneered by Schultz and co-workers are much more broadly enabling to the biochemical community.[44,45] These methods require the generation of an aminoacyl tRNA synthetase (RS) that is selective for an unnatural amino acid (Uaa). The UaaRS charges a cognate tRNA that recognizes the UAG stop codon ($tRNA_{CUA}$). The UAG stop codon is inserted into the gene for the protein target at the site of interest, while a different stop codon (e.g., UGA) is used for translation termination. After aminoacylation by the UaaRS, the $tRNA_{CUA}$ delivers the unnatural amino acid to the site of interest in the protein during ribosomal biosynthesis. Plasmids coding for the UaaRS, $tRNA_{CUA}$, and protein of interest are transformed into *E. coli*. After growth in the presence of the Uaa, protein containing the Uaa is purified for use in biochemical experiments. Because $tRNA_{CUA}$ must compete with release factors, protein production levels are lower than those for normal expression, but one can generally obtain 1−10 mg/L quantities of protein from cultures.[46]

A typical protein expression requires millimolar concentrations of the unnatural amino acid in the media. Thus, a highly efficient synthesis is required to produce the gram quantities of amino acid necessary for routine liter scale protein expression. Therefore, we began by designing a new synthesis of Acd starting from Tyr that is efficient in terms of labor and materials costs. This route also has the advantage of versatility, as substituted Acd derivatives can easily be prepared from Tyr analogs.

To obtain a UaaRS for incorporating Acd into proteins expressed in *E. coli*, we screened UaaRSs previously selected for incorporation of the structurally similar amino acids 4-(2′-bromoisobutyramido)phenylalanine (**2**, Brb, β) and *p*-benzoylphenylalanine (**3**, Bzf, ζ) shown in Figure 1.[47] Similar UaaRSs derived from *Methanococcus janaschii* TyrRS had been shown by the Mehl laboratory to be permissive of a variety of bulky

Figure 1. Unnatural amino acids used in this study. Aminoacyl tRNA synthetases (RSs) were screened for successful incorporation of acridon-2-ylalanine (**1**, Acd, δ) from an RS pool previously selected for incorporation of 4-(2′-bromoisobutyrlamido)phenylalanine (**2**, Brb, β) and *p*-benzoylphenylalanine (**3**, Bzf, ζ).

Tyr analogues; therefore, we suspected that these UaaRSs could accept Acd.[48,49] Indeed, we identified a useful synthetase from this library and characterized its efficiency of incorporation of Acd into model proteins. We also analyzed a series of mutants containing some active site residues from these selected UaaRSs and found that selectivity for Acd over Tyr depends upon a few key mutations.

In order to provide other investigators with important photophysical parameters for the use of Acd, we have characterized its quenching by several natural amino acids through Stern−Volmer titrations and determined the Förster radius, or distance of half-maximal energy transfer (R_0), for FRET to common fluorophores such as BODIPY Fl and fluorescein. Finally, we expressed several proteins to demonstrate the usage of Acd fluorescence in monitoring conformational changes and protein binding to peptide or ions through steady state or fluorescence lifetime measurements.

RESULTS AND DISCUSSION

Although we relied on a previously published synthetic route for our earlier experiments, when we began to contemplate in vivo incorporation, the large quantities of Acd required for expression in bacterial culture led us to consider a more cost-effective route. Acd syntheses reported by Lankiewicz and Sisido used *p*-nitrophenylalanine as the starting material.[38,39] After hydrogenation, *N*-Boc-*p*-aminophenylalanine ester was coupled to 2-iodobenzoic acid in an Ullman amine synthesis to give a product like **6**. Acid-catalyzed Friedel−Crafts cyclization in polyphosphoric acid (PPA) gave Acd (**1**). Further protecting group manipulations were used to obtain Acd in an appropriate form for peptide coupling or in vitro aminoacylation of tRNA.[38,39] We wished to improve the synthesis by starting from the natural amino acid Tyr and using a Buchwald−Hartwig coupling to the commodity chemical *O*-methyl anthranilate (**5**) to form **6**.[50] We also found heating in sulfuric acid with the addition of water to be a preferable way to induce Friedel−Crafts cyclization, as it resulted in deprotection of the Boc group and methyl esters as well the formation of Acd. Since preparation of **4** is straightforward, the efficiency of the route in Scheme 1 relied on developing a high yielding cross-coupling reaction.

In order to identify optimal conditions for the Pd-catalyzed coupling of **4** and **5**, we screened a number of combinations of solvent, temperature, base, and Pd/ligand ratios. From these experiments, we determined that the highest yields were obtained in 4 h at 120 °C with 5.2 mol % $Pd(OAc)_2$, 3.75 mol % racemic 2,2′-bis(diphenyl-phosphino)-1,1′-binaphthyl (*rac*-BINAP), and 3.0 equiv Cs_2CO_3 as base in cyclopentyl methyl ether (CPME). The results of our screen are shown in Supporting Information.

Scheme 1. Optimized Synthesis of Acridon-2-ylalanine

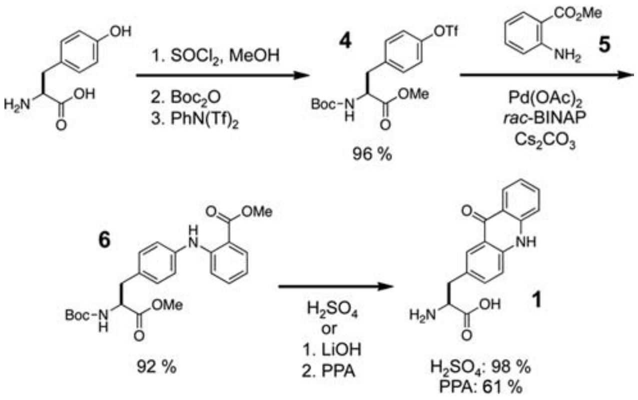

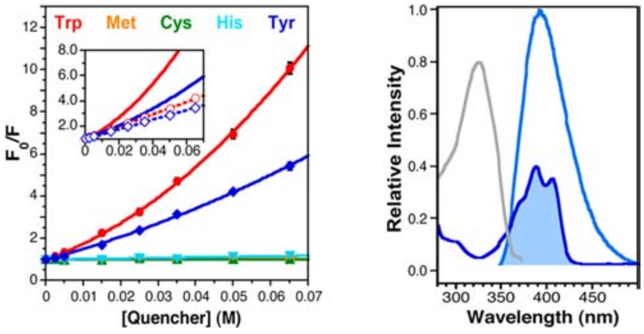

Figure 2. Acridon-2-ylalanine chromophore interactions. Left: Quenching by natural amino acids assessed through steady state fluorescence Stern–Volmer titrations with five amino acids: Trp (filled red circles), Met (orange squares), Cys (green upright triangles), His (pale blue downward triangles), Tyr (filled dark blue diamonds). Tyr methyl ester used for solubility, all other amino acids used as free acid. Left inset: Fluorescence lifetime Stern–Volmer titrations with Trp (open red circles) and Tyr (open dark blue diamonds). Steady state data shown as solid lines for comparison. Right: Absorbance (gray) and fluorescence emission (light blue) of Mcm and absorbance of Acd (blue), with spectral overlap shaded. Absorbance spectra are normalized by extinction coefficient; the emission spectrum scaling is arbitrary.

After screening in microplates was done, we carried out reactions on 250 mg and 1 g of **4** to ensure that our yields could translate to those scales. We found that 92% yields could be obtained from the optimal conditions, at a larger scale with toluene as the solvent (chosen based on cost since results were comparable to CPME), 135 °C heating, and a 23 h reaction time. Friedel–Crafts cyclization and global deprotection could be achieved in 98% yield, giving 87% overall yields of Acd on the 1 g scale.

In order to understand how best to use Acd, we began by assessing its sensitivity to local environment. This is clearly important if one wishes to use Acd as a probe of protein environment, but it is also an important background correction for those who wish to use Acd in PET or FRET studies. Acd has previously been shown to have an inherent solvatochromic response.[39] Its spectral shape blue shifts and its quantum yield changes from 0.95 to 0.29 on moving from water to THF. However, quenching of fluorophores by specific amino acids can also lead to environmental sensitivity.[51,52] As noted above, we have recently shown that Acd fluorescence can be quenched by a thioamide through a PET mechanism.[37] To determine the effects of natural amino acids on Acd fluorescence, we performed Stern–Volmer titrations with the common redox-active amino acids: Trp, Tyr, Met, Cys, and His. As seen in Figure 2, only Trp and Tyr quench Acd significantly.

Comparisons of data from steady state and fluorescence lifetime measurements indicate that Trp and Tyr quench Acd through a PET mechanism with both static (i.e., a nonemissive ground state complex is formed) and dynamic (i.e., excited state electron transfer) components. This can be seen in the Figure 2 inset where the dotted lines show the dynamic component observed in lifetime measurements made by time-correlated single photon counting (TCSPC).[53] Since Acd is quenched by Trp and Tyr, it should be sensitive to protein motions that change the proximity of these residues.

Acd can also function as a FRET acceptor for Trp because the tail of the Trp emission spectrum overlaps significantly with Acd absorbance (see Figure S2, Supporting Information). The Förster radius for this FRET pair is 23 Å, making it useful in monitoring distance changes in the 13–37 Å range. Since Trp can also act as a quencher of Acd through PET, care must be taken in interpreting FRET measurements at short distances (<15 Å) where both processes may be operative. To form a selectively excitable FRET pair, Acd can act as an acceptor for 7-methoxycoumarinylalanine (Mcm). For the Mcm/Acd pair, R_0 is 25 Å, making them useful in the 15–45 Å range. Acd can also function as a FRET donor with many common organic fluorophores such as carboxyfluorescein (R_0 = 51 Å), BODIPY Fl (R_0 = 49 Å), rhodamine 6G (R_0 = 49 Å), or nitrobenzodioxazole (NBD, R_0 = 37 Å). (The spectra used to determine these values are given in Figures S2–S4 in Supporting Information.) These values were calculated using a donor quantum yield (Φ_D) of 0.95 for Acd. Since, as we have just shown, Acd quantum yield can vary with local environment, any Acd FRET donor experiment must be compared to an equivalent experiment with an Acd label alone to correct for these effects on Acd Φ_D.

Although Sisido and co-workers had previously shown that Acd could be incorporated into proteins by in vitro ribosomal synthesis, we wished to produce milligram quantities of protein for biophysical studies. Therefore, we sought to obtain a UaaRS that would allow us to incorporate Acd in vivo.[38] Since Acd is significantly larger than Tyr, we began not by selecting from mutant TyrRS but by screening a library of synthetase mutants already selected for incorporation of Brb, Bzf, or 2-napthylalanine (Nap). It had previously been shown that for some amino acids that deviate substantially from the starting structure, it can be difficult to alter the binding pocket sufficiently to recognize the new amino acid in a single round of mutagenesis.[30] We also were intrigued by the idea that since selection protocols only include negative selection against natural amino acids, mutations that "open up" the binding pocket could lead to synthetases that are generally permissive of bulky unnatural amino acids, yet still selective against all of the natural amino acids.[48,49,54,55] Since these UaaRSs would not be challenged by multiple unnatural amino acids simultaneously, in theory, they would have perfectly adequate fidelity for protein production.

Screening was carried out by directing incorporation to a TAG site at position 150 in GFP and assessing the fluorescence of suspended cells (see Figure 3). Measured fluorescence reports on the production of full-length GFP, which indicates the ability of the synthetase to charge $tRNA_{CUA}$ with some amino acid, either Acd or a natural amino acid. Comparison of GFP production in cultures with Acd to cultures with only the

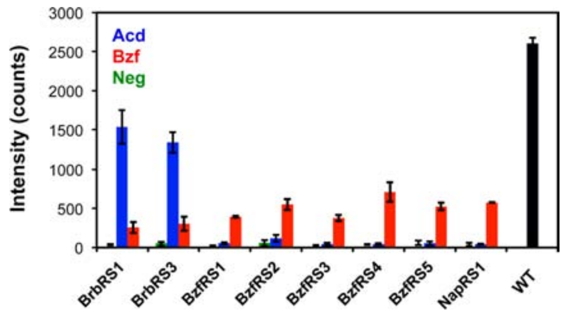

Figure 3. Synthetase selection and confirmation of Acd incorporation. Protein expression levels determined from fluorescence of GFP reporter construct containing a TAG stop codon at position 150. Fluorescence from full-length GFP indicates successful incorporation of an amino acid (Acd or Bzf) from a charged $tRNA_{CUA}$. Comparison to expressions containing only proteinogenic amino acids indicates UaaRS fidelity (Neg). Fluorescence from WT GFP (black) is shown as a positive control.

natural amino acids reports on the selectivity of the synthetase against Tyr. Although none of the BzfRSs or NapRSs showed evidence of noticeable Acd incorporation, we found that BrbRS1 and BrbRS3 could efficiently incorporate Acd while excluding Tyr. It is interesting that the NapRS was able to charge $tRNA_{CUA}$ with Bzf but not Acd. This may be attributable to the absence of Glu_{65} in the NapRS, which may interact with the acridone N−H. The active site sequences of all screened RS mutants are given in Supporting Information. Since BrbRS1 showed higher levels of protein expression, we used it for all subsequent Acd incorporation and refer to it as AcdRS.

We were curious to understand how AcdRS could be permissive of Brb and Acd, yet selective against Tyr. AcdRS contains five mutations relative to the parent *M. janaschii* TyrRS. We found that a single mutation of $Glu_{65}Val$ was sufficient to remove its ability to exclude Tyr (see Figure S8, Supporting Information). Similar results have been observed by Tipmann for other UaaRSs.[56] This is probably generally true of TyrRS variants evolved for the incorporation of large amino acids. The pocket must be large enough to accommodate the Uaa and yet not permit Tyr to bind with hydrating water molecules. It is perhaps not surprising that such a balance is easily broken. Additionally, we found evidence of misincorporation of *N*-phenyl-*p*-aminophenylalanine (Npf) resulting from decarboxylation during the global deprotection/cyclization step of Acd synthesis (see Figure S13, Supporting Information). This was true even when Npf was present as only a trace (<1% by HPLC) impurity in the Acd batch (see Figure S13, Supporting Information). Since this byproduct, which is difficult to remove by silica chromatography, is more likely to be obtained using sulfuric acid, a two-step protocol was adopted with saponification using LiOH followed by PPA cyclization (54% overall yield). Protein expressed using Acd batches from this PPA route consistently yielded pure protein containing no Npf at the site of interest (see Figure S14, Supporting Information). Efforts are currently underway to carry out negative selections to eliminate Npf misincorporation.

Once this synthetase mutant was identified, we tested incorporation by expressing Acd mutants of α-synuclein (αS, see Supporting Information), triose phosphate isomerase (TIM), and calmodulin (CaM) in *E. coli*. PAGE gel analysis and mass spectra confirming incorporation of Acd in these proteins are given in Supporting Information (Figure S12 and Table S1). In general, we obtained yields of purified protein that ranged from as low as 3% to as high as 69% of the yields of an equivalent expression of the wild type (WT) protein. While this variation may seem large, it is consistent with reports of changes in stop codon suppression efficiency with various proteins and positions.[42,43,57,58]

In order to demonstrate the utility of Acd as a fluorescent probe, we made several mutants of the Ca^{2+}-binding protein CaM, placing Acd at sites that were both buried and surface exposed (F_{13}, G_{41}, Y_{100}, and L_{113}). We chose CaM because it has been structurally characterized with a variety of substrates bound, and it has been extensively studied in biophysical experiments. All mutants were expressed in *E. coli* and purified by phenyl sepharose chromatography, and then their folding was assessed by circular dichroism (CD) spectroscopy with and without Ca^{2+}. The melting points (Tms), determined by thermal scans in the absence of Ca^{2+}, were within 5 °C of WT CaM (see Figure S16, Supporting Information). None of the mutants denatured in the presence of Ca^{2+}.

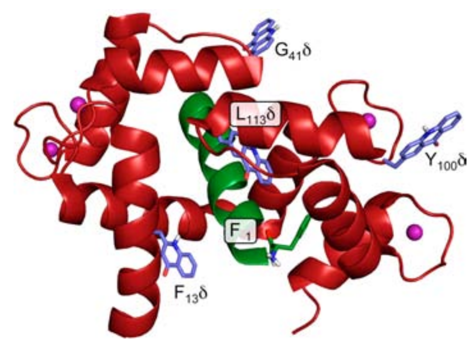

Figure 4. Calmodulin (CaM) labeling sites. An image showing Acd (blue) at position 13, 41, 100, or 113 in CaM (red) and highlighting position 1 in the pOCNC peptide (green). Ca^{2+} ions are shown as purple spheres. Adapted from PDB 1SYD using PyMol (Schrödinger, LLC; New York, NY) and Spartan (Wavefunction, Inc.; Irvine, CA).[59]

We wished to use Acd to monitor conformational changes associated with the binding of helical peptides to CaM. First, we used native PAGE gel analysis to confirm that Acd mutation did not disrupt the binding of our target peptide, pOCNC (H_2N-FRRIARLVGVLREFAFR-$CONH_2$). This peptide is derived from an olfactory cyclic nucleotide gated ion channel. The CaM/pOCNC structure has been previously determined by NMR.[59] Its binding affinity to WT CaM is 3 nM; therefore, we expected that only significant alterations in CaM structure would disrupt binding at 1−10 μM.[60] Indeed, all four Acd mutants bound a labeled derivative of pOCNC (see Figure S15, Supporting Information).

We then analyzed the fluorescence emission spectra of 10 μM CaM with varying concentrations of pOCNC. The fluorescence emission of CaM-$F_{13}\delta$, CaM-$Y_{100}\delta$, and CaM-$L_{113}\delta$ were unchanged, implying that Acd does not change environment during the binding of pOCNC (see Figure S18, Supporting Information). However, in its unbound form, CaM-$G_{41}\delta$ showed a blue shift in fluorescence relative to free Acd, and this blue shift went away as pOCNC was added to the solution (see Figure S18, Supporting Information). Previous photophysical characterization of Acd by Szymanska et al. has shown that Acd emission undergoes a blue shift in nonpolar environments. Since polycyclic aromatic molecules have been shown to bind in the helical cleft of CaM, we believe that the change in Acd emission occurs because pOCNC binding forces the Acd residue to move from a hydrophobic pocket into solvent.[61−63] While solvatochromic effects at position 41 could be used to monitor peptide binding to CaM, they complicate the interpretation of FRET data, so we focused our attention on the other positions.

To demonstrate the use of Acd as a FRET acceptor for Trp and Mcm, we synthesized variants of pOCNC labeled at the N-terminus with these fluorophores. The CaM Acd mutants were each titrated with Trp-pOCNC or Mcm-pOCNC, and fluorescence emission recorded from 350 to 550 nm while exciting at 295 nm (Trp) or 325 nm (Mcm). Binding data for Mcm-pOCNC and CaM-$L_{113}\delta$ are shown in Figure 5. We see a decrease in Mcm emission and an increase in Acd emission due to FRET. These data, obtained using 1 μM CaM, can be fit to obtain a dissociation constant of ≤9 nM. This is slightly higher than the 3 nM K_d previously reported for pOCNC, but this may reflect the changes in our system (a shorter peptide than that used in Liu et al., as well as Mcm and Acd labels).[60] The binding affinity is consistent with low nanomolar K_d values previously reported for natural and synthetic helical peptides as well as mutants of CaM that alter the hydrophobic packing of the peptide-binding pocket.[64−67]

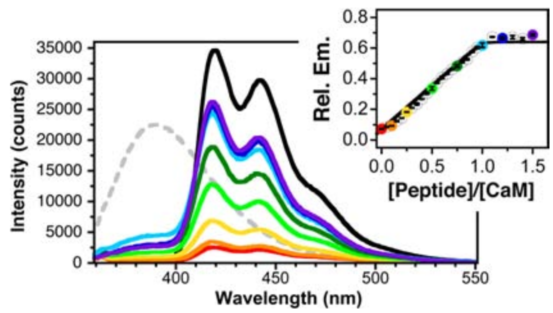

Figure 5. Monitoring CaM binding by FRET. Fluorescence spectra of 1 μM CaM-$L_{113}\delta$ in the presence of 0, 0.1, 0.25, 0.5, 0.75, 1.0, 1.2, or 1.5 equiv of Mcm-pOCNC, colored red, orange, yellow, light green, dark green, aqua, blue, and purple, respectively. The fluorescence spectrum of 1 μM Mcm-pOCNC alone is shown in dashed gray. All of these spectra were recorded with excitation at 325 nm. The spectrum with 1.5 equiv of Mcm-pOCNC is a difference spectrum in which the emission from 0.5 μM Mcm-pOCNC was subtracted from the spectrum of the 15 μM Mcm-pOCNC/10 μM CaM-$L_{113}\delta$ mixture. The fluorescence spectrum of 1 μM CaM-$L_{113}\delta$ alone with excitation at 385 nm is shown in black. Inset: Peptide binding monitored by changes in the emission at 442 nm due to excitation at 325 nm, normalized to direct Acd excitation at 385 nm. Additional data points at Mcm-pOCNC/CaM-$L_{113}\delta$ ratios of 0.05, 0.15, 0.2, 0.3, 0.35, 0.4, 0.45, 0.55, 0.6, 0.65, 0.7, 0.8, 0.85, 0.9, 0.95, 1.1, 1.3, and 1.4 are shown.

Several features of this experiment are important to note. First, we can see that binding reaches saturation in the 1:1 complex, as determined by examining the difference spectrum in which the emission from 0.5 equiv of Mcm-pOCNC was subtracted from the spectrum of the 1.5:1 Mcm-pOCNC/CaM-$L_{113}\delta$ mixture (purple trace in Figure 5). Second, FRET is efficient, as one would expect for a complex in which Mcm and Acd are separated by ~13 Å. For this separation, the theoretical FRET efficiency (E_{FRET}) is 0.97, which compares well to the measured E_{FRET} of 0.98, determined from the decrease in donor emission. Third, Mcm and Acd are a robust FRET pair, with minimal direct excitation of Acd at 325 nm (see red trace in Figure 5) and strong emission due to FRET (emission in the 1:1 complex is about half of the emission resulting from direct excitation of CaM-$L_{113}\delta$ at 385 nm). Similar results were obtained with binding Mcm-pOCNC to CaM-$F_{13}\delta$ and CaM-$Y_{100}\delta$ (see Figure S19, Supporting Information). As one can see in Table 1, The excellent quantitative agreement of the expected and observed E_{FRET} gives us confidence in using the Mcm/Acd FRET pair to study protein folding.

Table 1. FRET in CaM/Mcm-pOCNC Complexes

CaM mutants	E_Q obsvd[a]	R (Å)[b]	E_Q calcd[c]
CaM-$F_{13}\delta$	0.92	16	0.91
CaM-$Y_{100}\delta$	0.81	18	0.81
CaM-$L_{113}\delta$	0.98	13	0.97

[a] E_Q determined from quenching in 1:1 CaM/Mcm-pOCNC complex. [b] R is an average value calculated from the twenty lowest energy structures in PDB ID 1SYD using the positions of the corresponding amino acids.[59] [c] Φ_D of 0.098 determined for Mcm-pOCNC in 1:1 complex with CaM by measurement of the fluorescence of equimolar concentrations of free Mcm-pOCNC, and 1:1 CaM/Mcm-pOCNC. Mcm-pOCNC Φ_D assumed to be 0.18, the value for free Mcm.[68] R_0 for Mcm/Acd calculated using Φ_D of 0.098 is 23 Å.

Binding of Trp-pOCNC to any of the three CaM mutants can also be monitored by FRET (see Figure S20/21, Supporting Information). In this case, no background subtraction is necessary for superstoichiometric complexes since Trp has no fluorescence emission above 400 nm. However, there is substantial direct excitation of Acd upon irradiation at 295 nm (27% of the emission due to excitation at 385 nm). Since there is also a possibility of Trp quenching of Acd emission through PET, we are hesitant to interpret E_{FRET} data in terms of distances for Trp in the same way that we do for Mcm. In addition, most proteins contain more than one Trp, so FRET data would need to be fit to complex models with more than one donor fluorophore. Regardless, Trp FRET can still easily be used to quantify protein−protein binding energies by fitting concentration-dependent data. One of the protein partners could be WT, provided that it contained at least one Trp residue. As noted above, Trp and Mcm each have benefits and drawbacks as Acd FRET donors. Since some quenching may occur via PET to Trp, we view Mcm as a more optimal FRET donor. However, many researchers may find Trp/Acd FRET pairs more useful due to the ease of genetically encoding doubly labeled proteins.

In addition to singlet energy transfer interactions with organic chromophores like Trp or Mcm, Acd can undergo intersystem crossing to donate energy to lanthanide ions such as Eu^{3+}.[41] While this has previously been demonstrated in short, synthetic peptides, the ability to genetically encode Acd allows us to implement the same Eu^{3+} LRET probes in proteins expressed in *E. coli*. To demonstrate Acd-sensitized Eu^{3+} emission, we relied on the precedent for CaM binding a variety of cations, including the lanthanides Tb^{3+} and Eu^{3+}.[69−71] Since efficient LRET typically requires close contact between the donor chromophore and lanthanide ion, we chose CaM-$Y_{100}\delta$ as a construct for LRET studies because Y_{100} is adjacent to both C-terminal binding sites. Titration of CaM-$Y_{100}\delta$ with $Eu(NO_3)_3$ revealed a dose-dependent increase in Eu^{3+} emission at 592 and 615 nm. The 615 nm emission data could be fit to a two site binding model with K_d's of 28 μM and 154 μM and Hill coefficients of 1.1 and 2.6, respectively. The 615 nm signal primarily derives from the lower-affinity binding event(s), which presumably corresponds to binding at the C-terminus, particularly to site III, defined by residues D_{94}, D_{96}, N_{98}, Y_{100}, S_{102}, and E_{105}. Previous experiments have found higher affinity (K_d = 1 μM) binding of lanthanides to this site; the lower affinity observed here may be due to disruption by the Acd residue, as studies have found that minor mutations at site III can dramatically decrease Ca^{2+} affinity.[72−74] For higher specificity LRET labeling, one may use lanthanide-binding sequences of the type described by Imperiali and co-workers.[13,75]

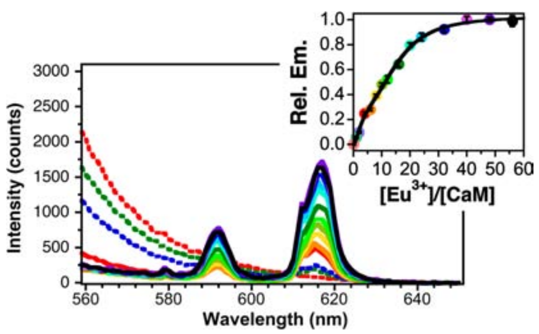

Figure 6. Monitoring Eu^{3+} Binding to CaM By LRET. Luminescence emission spectra of 10 μM CaM-$Y_{100}\delta$ in the presence of 0, 1, 2, 5, 6, 8, 10, 12, 16, 20, 24, 32, 40, 48, 56 equiv of $EuNO_3$, colored dashed red, dashed green, dashed blue, red, orange, yellow, chartreuse, light green, dark green, aqua, light blue, dark blue, light purple, dark purple, and black, respectively. Spectra recorded with excitation at 385 nm. Inset: Eu^{3+} binding monitored by changes in the emission at 615 nm. Data fit to two cooperative binding transitions as described in Supporting Information.

In many proteins, specific quenching interactions with a nearby Trp or Tyr may occur, as implicated by our Stern−Volmer experiments. These could be engineered into either peptide or protein binding partners, and Acd quenching could be used to monitor bimolecular interactions. Indeed, we have shown that this is the case for Acd mutants of TIM. TIM forms a dimer as shown in Figure 7.[76,77] We selected Phe_{74} and Tyr_{101} as positions for Acd incorporation since they approach each other at the dimer interface and they are relatively far (≥13 Å) from the other Trp and Tyr residues.

The single mutants TIM-$F_{74}\delta$ and TIM-$Y_{101}\delta$ were purified, and fluorescence spectra were acquired in varying concentrations of urea. In the absence of urea, both mutants are quenched relative to the fluorescence of an equimolar concentration Acd (urea had no effect on the fluorescence of free Acd). TIM-$F_{74}\delta$ is quenched to a greater degree, as one would expect, since it is in contact with Tyr_{101} of the other TIM monomer unit in the folded, dimeric native state of TIM. The TIM-$Y_{101}\delta$ mutant, on the other hand, places no Trp or Tyr in direct contact with Acd. The two mutants recover comparable levels of fluorescence upon titration with urea, since quenching by Tyr_{101} is relieved as TIM unfolds and dimer dissociation occurs. In addition to monitoring unfolding by changes in steady-state fluorescence, we also find it useful to measure quenching by changes in the fluorescence lifetime of Acd. Lifetime-based measurements of quenching made by TCSPC are very valuable, because they are not sensitive to concentration matching like steady-state measurements.[53] Consistent with our steady state data, we observe a decrease in Acd lifetime in both TIM-$F_{74}\delta$ and TIM-$Y_{101}\delta$ relative to free Acd: τ_{Avg}(free) = 15.8 ns, τ_{Avg}(TIM-$F_{74}\delta$) = 6.8 ns, and τ_{Avg}(TIM-$Y_{101}\delta$) = 12.7 ns. Lifetime measurements in 0, 2, 3, and 4 M urea demonstrate that the more dramatic Tyr-specific quenching in TIM-$F_{74}\delta$ is relieved by 3 M urea, and that global unfolding gives comparable lifetimes for both mutants in 4 M urea. These experiments show how changes in Acd lifetime, due either to general quenching phenomena and/or specific placement near a quenching residue, may be used to monitor unfolding.

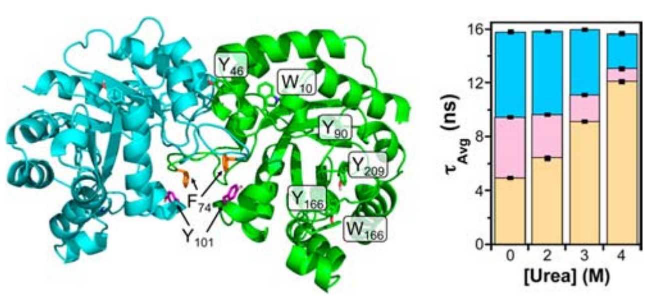

Figure 7. Triose phosphate isomerase (TIM) unfolding. Left: An image showing TIM dimer (protomers colored cyan and green) with Phe_{74} (orange) and Tyr_{101} (pink) highlighted in both protomers. Other Trp and Tyr residues in both protomers are shown in stick representation and are labeled in the green protomer. Image adapted from PDB 1TRE using PyMol (Schrödinger, LLC; New York, NY).[77] Right: Monitoring TIM unfolding monitored by changes in average fluorescence lifetime for solutions of 2 μM TIM-$F_{74}\delta$ (orange), TIM-$Y_{101}\delta$ (magenta), or free Acd (blue) in 15 mM HEPES 140 mM KCl buffer with varying concentrations of urea. Acd lifetime derived from biexponential fits to the primary data. See Supporting Information for details.

■ CONCLUSIONS

The fluorescent unnatural amino acid Acd had previously been shown to be a useful probe of protein conformational change, but its use had been limited to synthetic peptides and in vitro translation. Here, we report an efficient and affordable synthesis of Acd, and the identification of an Acd-specific variant of the *M. janaschii* TyrRS. These developments allow one to easily produce milligram quantities of Acd-labeled proteins for biophysical studies. We have characterized the photophysical properties of Acd, including quenching interactions with select natural amino acids and FRET interactions with common fluorophores such as coumarin. We have also demonstrated the incorporation of Acd into several proteins and used changes in Acd fluorescence to monitor peptide binding and ion binding as well as protein folding.

Of course, the use of Acd as a probe of protein structure and function is not limited to the examples here. Acd quenching or FRET can also be used to monitor intramolecular conformational changes, either using a Trp/Acd FRET pair or an Mcm/Acd pair by labeling a Cys residue with a methoxycoumarin derivative. LRET applications using the optimized lanthanide-binding tags developed by the Imperiali group could enhance the utility of Acd-based LRET.

One of the advantages of our synthesis relative to previously published methods is its versatility. Some aspects of Acd photochemistry are nonideal, such as its low extinction coefficient and blue wavelength emission. In some experiments, its sensitivity to solvent may also be problematic. We would like to synthesize analogues of Acd that might exhibit improved photophysical properties. Fortunately, our synthetic route is compatible with analogues of Tyr and anthranilate that contain electron-withdrawing or electron-donating groups. The resulting Tyr analogues should have a "push-pull" chromophore that is more red-shifted and brighter than the parent Acd.[78−81]

Finally, since the AcdRS identified here can also charge $tRNA_{CUA}$ with Brb, we have undertaken crystallography studies to determine the structural basis for substrate binding. Our preliminary analysis indicates that Glu_{65} may be important and that selectivity toward Acd vs Tyr is conferred by a few residues. As noted within, this is not surprising for a synthetase that is permissive of several large amino acids. We are exploring the permissivity of the AcdRS toward other tricyclic scaffolds such as xanthones and acridines. We expect that many such fluorescent amino acids may be incorporable.

EXPERIMENTAL PROCEDURES

General Information. L-Tyrosine, thionyl chloride, di-*tert*-butyl dicarbonate (Boc anhydride), methyl 2-aminobenzoate, and phenyl-sepharose CL-4B resin were purchased from Sigma-Aldrich (St. Louis, MO, USA). *N*-Phenyl-bis(trifluoromethane sulfonimide) was purchased from Oakwood Chemical (West Columbia, SC, USA). $Eu(NO_3)_3$ came from Strem Chemicals (Newburyport, MA, USA). *E. coli* BL21(DE3) cells were purchased from Stratagene (La Jolla, CA, USA). *E. coli* ElectroMAX DH10B cells were purchased from Invitrogen (Grand Island, NY, USA). Milli-Q filtered (18 MΩ) water was used for all solutions (Millipore; Billerica, MA, USA). All peptide synthesis reaction vessels (RVs) were treated with Sigmacote prior to use.

DNA sequencing was performed at the University of Pennsylvania DNA sequencing facility. Matrix-assisted laser desorption ionization (MALDI) mass spectra were collected with a Bruker Ultraflex III MALDI-TOF-TOF mass spectrometer (Billerica, MA). UV/vis absorbance spectra were obtained with a Hewlett-Packard 8452A diode array spectrophotometer (currently Agilent Technologies; Santa Clara, CA). NMR spectra, ^1H and ^{13}C, were collected with a Bruker DRX 500 MHz instrument. $CDCl_3$ was calibrated at δ 7.27 for ^1H and δ 77.2 for ^{13}C. DEPT-135 Carbon NMR notation as follows: no signal is designated by (np), a positive signal is designated by (+), and a negative signal is designated by (−). High-resolution mass spectra (HRMS) were obtained on a Waters LC-TOF mass spectrometer (model LCT-XE Premier) using electrospray ionization in positive mode.

Methyl (*S*)-2-((*tert*-butoxycarbonyl)amino)-3-(4-(((trifluoromethyl)sulfonyl)oxy)phenyl)propanoate (4). Compound **4** was synthesized essentially as described. Characterization matched previous reports.[37,39]

(*S*)-Methyl 2-((4-(2-((*tert*-butoxycarbonyl)amino)-3-methoxy-3-oxopropyl)phenyl)amino)benzoate (6). 75 mL of toluene was degassed with argon for 15 min in a 250 mL flame-dried round-bottom flask. Tyr derivative **4** (3.000 g, 7.02 mmol) was added to the flask followed by methyl 2-aminobenzoate (1200 μL, 9.27 mmol). This solution was degassed with argon for 5 min. Then palladium(II) acetate (0.082 g, 0.365 mmol), and racemic 2,2′-bis(diphenyl-phosphino)-1,1′-binaphthyl (0.054 g, 0.087 mmol) were added to the flask. Cesium carbonate (6.88 g, 21.1 mmol) was ground and added to the flask. The flask was then fitted with a reflux condenser and heated to 135 °C for 23 h. After the solution was allowed to cool to ambient temperature, the contents were filtered through a short plug of silica gel using CH_2Cl_2 to transfer the material to the silica (250 mL) and then ethyl acetate (500 mL) was used to elute the product. The clarified solution was then concentrated under reduced pressure. Silica gel flash column chromatography (10% ethyl acetate in hexanes) afforded 2.759 g (6.44 mmol, 91.7%) of a pale yellow oil. R_f = 0.2 in 15% ethyl acetate in hexanes; ^1H NMR (500 MHz, $CDCl_3$) δ 9.44 (s, 1H), 7.96 (d, J = 8.0 Hz, 1H), 7.31 (t, J = 7.9 Hz, 1H), 7.23 (d, J = 8.5 Hz 1H), 7.18 (d, J = 8.2 Hz, 2H), 7.10 (d, J = 8.1 Hz, 1 H), 6.73 (t, J = 7.5 Hz, 1 H), 5.05 (d, J = 7.9 Hz, 1 H), 4.61 − 4.57 (m, 1 H), 3.90 (s, 3H), 3.74 (s, 3H), 3.07 (dd, J = 26.5, 5.7 Hz, 2 H), 1.43 (s, 9H); ^{13}C NMR (125 MHz, $CDCl_3$): δ 172.5 (np), 169.0 (np), 155.3 (np), 148.0 (np), 139.8 (np), 134.2 (+), 131.8 (+), 131.3 (np), 130.4 (+), 122.6 (+), 117.3 (+), 114.2 (+), 112.1 (np), 80.0 (np), 54.6 (+), 52.4 (+), 51.9 (+), 38.0 (−), 28.5 (+); HRMS (ESI) m/z calcd for $C_{23}H_{28}N_2O_6$ $[M + H]^+$ 429.2000, found 429.2026.

(*S*)-2-Amino-3-(9-oxo-9,10-dihydroacridin-2-yl) Propanoic Acid (Acd, 1). Twelve milliliters of 13.5 M sulfuric acid was added to a flask containing **6** (1.02 g, 2.38 mmol). The flask was then fitted with a reflux condenser and heated to 115 °C for 16 h in an oil bath. 80 mL of water was then added slowly to the flask and allowed to stir for 15 min. The reaction was then removed from the hot oil bath and allowed to cool with stirring. Upon reaching ambient temperature, the solution was then cooled to 4 °C and allowed to stand for 2 h. During the 2 h cooling period, 100 g of Dowex ion-exchange resin was made into a slurry with 1.8 M aqueous sulfuric acid and applied to a flash chromatography column. The resin was washed with 350 mL of 1.8 M aqueous sulfuric acid, 2 L of water, 1 L of 1.5 M aqueous ammonium hydroxide, and 4 L of water. Following these washes, the resin was dried by passing air through the column. The cooled Acd solution was then vacuum filtered on a Büchner funnel to remove precipitated material and the clarified solution was applied to the washed and dried ion-exchange resin. The resulting resin slurry was shaken in the chromatography column for 5 min before the solution was drained. This solution is then reapplied to the dried resin and shaken for an additional 5 min. The twice-passed solution was then set aside. The loaded resin was washed by 4 L of water before the compound of interest was eluted with 1.45 L of 1.5 M ammonium hydroxide. The solution was concentrated to 50 mL by rotary evaporation and then lyophilized to dryness, yielding a crop of Acd as a yellow powder (0.6375 g 2.26 mmol 94.9%). The ion-exchange resin was recycled by washing with 4 L of water and dried until further use. To maximize yield, the twice-passed solution was reapplied to washed and dried ion-exchange resin, and the process was repeated to yield a second crop of Acd (0.0232 g of 0.082 mmol 3.4%). Total yield for the two columns was 98.3% and purity was >98% by analytical HPLC. Characterization of this compound matched previous reports.[37] Saponification and polyphosphoric acid (PPA) cyclization procedures are given in Supporting Information.

Candidate Synthetase Screening. For screening of Acd incorporation, protein expressions were performed in DH10B cells transformed with pBad-sfGFP-150TAG and a synthetase-containing pDule vector to produce UAA-sfGFP as previously described.[39] Arabinose autoinduction media and method were used. UAAs were dissolved in sterile water with 1 mol equiv of aqueous NaOH and then added to the appropriate media to a final concentration of 1 mM. Negative control cultures of the mutant proteins, containing no UAA, were grown simultaneously. Cultures at 37 °C were inoculated with 1:100 dilution of saturated noninducing cultures. Standard expressions were performed in duplicate with 0.45 mL of media in a 96-well 2 mL culture plate with shaking and incubation at 37 °C. Fluorescence measurements of the cultures were collected 40 h after inoculation using a BioTek Synergy 2 microplate reader. The emission from 528 nm (20 nm bandwidth) with excitation at 485 nm (20 nm bandwidth). Samples were prepared by diluting suspended cells directly from culture 10-fold with phosphate buffer saline. To quantify the protein yield, DH10B *E. coli* cells cotransformed with the pBad-sfGFP-150TAG vector and the machinery plasmid pDule-RS were used to inoculate 5 mL of noninducing media containing 100 mg/mL ampicillin (Amp) and 25 mg/mL tetracycline (Tet). The noninducing media culture was grown to saturation with shaking at 37 °C and 1.5 mL was used to inoculate 150 mL of autoinduction media with 100 mg/mL Amp, 25 mg/mL Tet, and 1 mM Uaa. After 40 h of shaking with incubation at 37 °C, cells from 100 mL of culture were collected by centrifugation. The protein was purified using BD-TALON cobalt ion-exchange chromatography. Purified proteins were checked for concentration by Bradford protein assay.

Calmodulin Binding Assays. All peptide binding experiments were conducted in 15 mM HEPES buffer, 140 mM KCl, and 6 mM $CaCl_2$, pH 6.70. Dry peptides and lyophilized protein were brought up in a minimal amount of buffer to make fresh concentrated stock solutions for each experiment. Protein concentrations were determined by (1) use of Thermo Scientific's Pierce BCA protein assay kit using known concentrations of bovine serum albumin as the standard and (2) UV/vis absorbance measurements using Acd absorbance (ε_{386} = 5.700 $M^{-1}\cdot cm^{-1}$).[39] Mcm-pOCNC concentrations were determined using 7-methoxycoumarin absorbance (ε_{325} = 12 000 $M^{-1}\cdot cm^{-1}$).[68] Fluorescence spectra were obtained using a Photon Technologies International (PTI; Piscataway, NJ, USA) Quantamaster 40 fluorescence spectrometer. For titrations using CaM-$L_{113}\delta$ and Mcm-pOCNC, samples consisted of 1 μM CaM-$L_{113}\delta$ and increasing Mcm-pOCNC concentrations from 0.05 μM to 1.5 μM in 15 mM HEPES, 140 mM KCl and 6 mM $CaCl_2$, pH 6.70. The excitation wavelength was 325 nm, and emission spectra were collected from 350 to 550 nm. For titrations using CaM-$Y_{100}\delta$ and Eu^{3+}, samples consisted of 10 μM CaM-$Y_{100}\delta$ and increasing $Eu(NO_3)_3$ concentrations from 1.0 μM to 560 μM in 15 mM HEPES and 140 mM KCl at pH 6.70. The excitation wavelength was 386 nm, and emission spectra were collected from 400 to 650 nm. Instrument settings for these experiments were 1 nm slit widths at both the excitation and emission monochromators, 1 nm step size, and 1 s averaging time.

TIM Urea Assays. All unfolding experiments were conducted in 15 mM HEPES buffer and 140 mM KCl, pH 6.70 with varying concentrations of urea. After Ni-NTA column purification, the pure protein fractions were dialyzed three times against this buffer without urea. Protein concentrations were determined with a bicinchoninic acid (BCA) assay kit (Thermo Scientific Pierce) using solutions of bovine serum albumin (BSA) as standards. For each mutant, solutions were prepared that contained approximately 10 μM protein, and the appropriate concentration of urea was established by addition of various amounts of a 10 M urea, 15 mM HEPES, and 140 mM KCl buffer pH 6.70. Each sample was prepared in triplicate. Time-resolved fluorescence measurements were performed using the time-correlated single photon counting (TCSPC) method. The TCSPC system consisted of a blue diode laser (PicoQuant GmbH; Berlin, Germany) generating 10 MHz output pulses at 405 nm, a subtractive double monochromator with an MCP-PMT (Hamamatsu Photonics R2809U; Bridgewater, NJ), and a TCSPC computer board (Becker and Hickl SPC-630; Berlin, Germany). Emission at 450 nm was monitored. All samples were thermostatted at 25 °C. Data analysis was performed with FluoFit software (PicoQuant) as described in Supporting Information.

■ ASSOCIATED CONTENT

Ⓢ Supporting Information

Screening of conditions for Pd cross-coupling, additional synthetic procedures, steady state and lifetime Stern−Volmer fluorescence quenching experiments, protein mutagenesis, expression, and characterization, primary fluorescence data for CaM, TIM, and αS experiments. This material is available free of charge via the Internet at http://pubs.acs.org. Primary data used to generate figures and tables have been digitally archived and can be obtained by emailing the corresponding author.

■ AUTHOR INFORMATION

Corresponding Authors

ejpetersson@sas.upenn.edu
ryan.mehl@oregonstate.edu

Notes

The authors declare no competing financial interest.

■ ACKNOWLEDGMENTS

This work was supported by funding from the University of Pennsylvania, the Searle Scholars Program (10-SSP-214 to EJP), the National Institutes of Health (NIH NS081033 to E.J.P.), the National Science Foundation (NSF MCB-0448297 to R.A.M.), and the Cell Imaging and Analysis Facilities and Services Core of the EHSC, Oregon State University (P30 ES00210, NIEHS, NIH to R.A.M.). Instruments were supported by the NSF and NIH include HRMS (NIH RR-023444) and MALDI-MS (NSF MRI-0820996). We thank Dr. Simon Berritt of the UPenn/Merck High Throughput Experimentation (HTE) Laboratory (NSF GOALI CHE-0848460) for assistance with reaction screening. The HTE Laboratory is thankful for the donations of Accelrys Library Studio and Virscidian Analytical Studio software. We also thank Dr. Christopher Lanci of the UPenn Biological Chemistry Resource Center for assistance with automated peptide synthesis and circular dichroism spectroscopy (supported by UPenn Laboratory for Research on the Structure of Matter with NSF MRSEC DMR 0520020, 1120901). L.C.S. thanks Professor Eric J. Schelter (UPenn) for $Eu(NO_3)_3$. J.M.G. thanks Tom Troxler of the Ultrafast Optical Processes Laboratory (NIH 9P41GM104605) for assistance with TCSPC measurements.

■ REFERENCES

(1) Doose, S.; Neuweiler, H.; Sauer, M. *ChemPhysChem* **2009**, *10*, 1389−1398.
(2) dos Remedios, C. G.; Moens, P. D. J. *J. Struct. Biol.* **1995**, *115*, 175−185.
(3) Eftink, M. R. *Methods Biochem. Anal.* **1991**, *35*, 127−205.
(4) Stryer, L.; Haugland, R. P. *Proc. Natl. Acad. Sci. U. S. A.* **1967**, *58*, 719−726.
(5) Wu, P.; Brand, L. *Anal. Biochem.* **1994**, *218*, 1−13.
(6) Chalfie, M.; Tu, Y.; Euskirchen, G.; Ward, W. W.; Prasher, D. C. *Science* **1994**, *263*, 802−805.
(7) Piston, D. W.; Kremers, G. J. *Trends Biochem. Sci.* **2007**, *32*, 407−414.
(8) Tsien, R. Y. *Annu. Rev. Biochem.* **1998**, *67*, 509−544.
(9) Sletten, E. M.; Bertozzi, C. R. *Angew. Chem., Int. Ed.* **2009**, *48*, 6974−6998.
(10) Giepmans, B. N. G.; Adams, S. R.; Ellisman, M. H.; Tsien, R. Y. *Science* **2006**, *312*, 217−224.
(11) Hinner, M. J.; Johnsson, K. *Curr. Opin. Biotechnol.* **2010**, *21*, 766−776.
(12) Chen, I.; Howarth, M.; Lin, W. Y.; Ting, A. Y. *Nat. Methods* **2005**, *2*, 99−104.
(13) Franz, K. J.; Nitz, M.; Imperiali, B. *ChemBioChem* **2003**, *4*, 265−271.
(14) Griffin, B. A.; Adams, S. R.; Tsien, R. Y. *Science* **1998**, *281*, 269−272.
(15) Gronemeyer, T.; Chidley, C.; Juillerat, A.; Heinis, C.; Johnsson, K. *Protein Eng. Des. Sel.* **2006**, *19*, 309−316.
(16) Hoffmann, C.; Gaietta, G.; Zurn, A.; Adams, S. R.; Terrillon, S.; Ellisman, M. H.; Tsien, R. Y.; Lohse, M. J. *Nat. Protoc.* **2010**, *5*, 1666−1677.
(17) Keppler, A.; Gendreizig, S.; Gronemeyer, T.; Pick, H.; Vogel, H.; Johnsson, K. *Nat. Biotechnol.* **2003**, *21*, 86−89.
(18) Los, G. V.; Encell, L. P.; McDougall, M. G.; Hartzell, D. D.; Karassina, N.; Zimprich, C.; Wood, M. G.; Learish, R.; Ohane, R. F.; Urh, M.; Simpson, D.; Mendez, J.; Zimmerman, K.; Otto, P.; Vidugiris, G.; Zhu, J.; Darzins, A.; Klaubert, D. H.; Bulleit, R. F.; Wood, K. V. *ACS Chem. Biol.* **2008**, *3*, 373−382.
(19) Luedtke, N. W.; Dexter, R. J.; Fried, D. B.; Schepartz, A. *Nat. Chem. Biol.* **2007**, *3*, 779−784.
(20) Miller, L. W.; Cai, Y. F.; Sheetz, M. P.; Cornish, V. W. *Nat. Methods* **2005**, *2*, 255−257.
(21) Yin, J.; Straight, P. D.; McLoughlin, S. M.; Zhou, Z.; Lin, A. J.; Golan, D. E.; Kelleher, N. L.; Kolter, R.; Walsh, C. T. *Proc. Natl. Acad. Sci. U. S. A.* **2005**, *102*, 15815−15820.
(22) Zhou, Z.; Koglin, A.; Wang, Y.; McMahon, A. P.; Walsh, C. T. *J. Am. Chem. Soc.* **2008**, *130*, 9925−9930.
(23) Popp, M. W.; Antos, J. M.; Grotenbreg, G. M.; Spooner, E.; Ploegh, H. L. *Nat. Chem. Biol.* **2007**, *3*, 707−708.

(24) Saraogi, I.; Zhang, D. W.; Chandrasekaran, S.; Shan, S. O. *J. Am. Chem. Soc.* **2011**, *133*, 14936−14939.
(25) Cornish, V. W.; Benson, D. R.; Altenbach, C. A.; Hideg, K.; Hubbell, W. L.; Schultz, P. G. *Proc. Natl. Acad. Sci. U. S. A.* **1994**, *91*, 2910−2914.
(26) Hohsaka, T.; Abe, R.; Shiraga, K.; Sisido, M. *Nucleic Acids Res.* **2003**, 271−272.
(27) Kajihara, D.; Abe, R.; Iijima, I.; Komiyama, C.; Sisido, M.; Hohsaka, T. *Nat. Methods* **2006**, *3*, 923−929.
(28) Taki, M.; Hohsaka, T.; Murakami, H.; Taira, K.; Sisido, M. *J. Am. Chem. Soc.* **2002**, *124*, 14586−14590.
(29) Pantoja, R.; Rodriguez, E. A.; Dibas, M. I.; Dougherty, D. A.; Lester, H. A. *Biophys. J.* **2009**, *96*, 226−237.
(30) Lee, H. S.; Guo, J.; Lemke, E. A.; Dimla, R. D.; Schultz, P. G. *J. Am. Chem. Soc.* **2009**, *131*, 12921−12923.
(31) Summerer, D.; Chen, S.; Wu, N.; Deiters, A.; Chin, J. W.; Schultz, P. G. *Proc. Natl. Acad. Sci. U. S. A.* **2006**, *103*, 9785−9789.
(32) Wang, J.; Xie, J.; Schultz, P. G. *J. Am. Chem. Soc.* **2006**, *128*, 8738−8739.
(33) Chatterjee, A.; Guo, J. T.; Lee, H. S.; Schultz, P. G. *J. Am. Chem. Soc.* **2013**, *135*, 12540−12543.
(34) Kalstrup, T.; Blunck, R. *Proc. Natl. Acad. Sci. U. S. A.* **2013**, *110*, 8272−8277.
(35) Parrish, A. R.; She, X. Y.; Xiang, Z.; Coin, I.; Shen, Z. X.; Briggs, S. P.; Dillin, A.; Wang, L. *ACS Chem. Biol.* **2012**, *7*, 1292−1302.
(36) Shen, B.; Xiang, Z.; Miller, B.; Louie, G.; Wang, W. Y.; Noel, J. P.; Gage, F. H.; Wang, L. *Stem Cells* **2011**, *29*, 1231−1240.
(37) Goldberg, J. M.; Speight, L. C.; Fegley, M. W.; Petersson, E. J. *J. Am. Chem. Soc.* **2012**, *134*, 6088−6091.
(38) Hamada, H.; Kameshima, N.; Szymanska, A.; Wegner, K.; Lankiewicz, L.; Shinohara, H.; Taki, M.; Sisido, M. *Bioorg. Med. Chem.* **2005**, *13*, 3379−3384.
(39) Szymanska, A.; Wegner, K.; Lankiewicz, L. *Helv. Chim. Acta* **2003**, *86*, 3326−3331.
(40) Reynolds, A. M.; Sculimbrene, B. R.; Imperiali, B. *Bioconjugate Chem.* **2008**, *19*, 588−591.
(41) Dadabhoy, A.; Faulkner, S.; Sammes, P. G. *J. Chem. Soc. Perkin 2* **2002**, 348−357.
(42) Albayrak, C.; Swartz, J. R. *Nucleic Acids Res.* **2013**, *41*, 5949−5963.
(43) Goerke, A. R.; Swartz, J. R. *Biotechnol. Bioeng.* **2009**, *102*, 400−416.
(44) Wang, L.; Brock, A.; Herberich, B.; Schultz, P. G. *Science* **2001**, *292*, 498−500.
(45) Wang, L.; Schultz, P. G. *Angew. Chem., Int. Ed.* **2005**, *44*, 34−66.
(46) Young, T. S.; Ahmad, I.; Yin, J. A.; Schultz, P. G. *J. Mol. Biol.* **2010**, *395*, 361−374.
(47) Peeler, J. C.; Woodman, B. F.; Averick, S.; Miyake-Stoner, S. J.; Stokes, A. L.; Hess, K. R.; Matyjaszewski, K.; Mehl, R. A. *J. Am. Chem. Soc.* **2010**, *132*, 13575−13577.
(48) Miyake-Stoner, S. J.; Refakis, C. A.; Hammill, J. T.; Lusic, H.; Hazen, J. L.; Deiters, A.; Mehl, R. A. *Biochemistry* **2010**, *49*, 1667−1677.
(49) Stokes, A. L.; Miyake-Stoner, S. J.; Peeler, J. C.; Nguyen, D. P.; Hammer, R. P.; Mehl, R. A. *Mol. Biosys.* **2009**, *5*, 1032−1038.
(50) Wolfe, J. P.; Wagaw, S.; Marcoux, J. F.; Buchwald, S. L. *Acc. Chem. Res.* **1998**, *31*, 805−818.
(51) Chen, H.; Ahsan, S. S.; Santiago-Berrios, M. E. B.; Abruña, H. D.; Webb, W. W. *J. Am. Chem. Soc.* **2010**, *132*, 7244−7245.
(52) Chen, Y.; Barkley, M. D. *Biochemistry* **1998**, *37*, 9976−9982.
(53) Lakowicz, J. R. *Principles of Fluorescence Spectroscopy*; Springer: New York, 2006.
(54) Young, D. D.; Jockush, S.; Turro, N. J.; Schultz, P. G. *Bioorg. Med. Chem. Lett.* **2011**, *21*, 7502−7504.
(55) Young, D. D.; Young, T. S.; Jahnz, M.; Ahmad, I.; Spraggon, G.; Schultz, P. G. *Biochemistry* **2011**, *50*, 1894−1900.
(56) Antonczak, A. K.; Simova, Z.; Yonemoto, I. T.; Bochtler, M.; Piasecka, A.; Czapinska, H.; Brancale, A.; Tippmann, E. M. *Proc. Natl. Acad. Sci. U. S. A.* **2011**, *108*, 1320−1325.
(57) Miller, J. H.; Albertini, A. M. *J. Mol. Biol.* **1983**, *164*, 59−71.
(58) Pedersen, W. T.; Curran, J. F. *J. Mol. Biol.* **1991**, *219*, 231−241.
(59) Contessa, G. M.; Orsale, M.; Melino, S.; Torre, V.; Paci, M.; Desideri, A.; Cicero, D. O. *J. Biomol. NMR* **2005**, *31*, 185−199.
(60) Liu, M. Y.; Chen, T. Y.; Ahamed, B.; Li, J.; Yau, K. W. *Science* **1994**, *266*, 1348−1354.
(61) Barnes-Seeman, D.; Park, S. B.; Koehler, A. N.; Schreiber, S. L. *Angew. Chem., Int. Ed.* **2003**, *42*, 2376−2379.
(62) Menyhard, D. K.; Keseru, G. M.; Naray-Szabo, G. *Curr. Comput.-Aided Drug Des.* **2009**, *5*, 264−279.
(63) Yin, H.; Frederick, K. K.; Liu, D. H.; Wand, A. J.; DeGrado, W. F. *Org. Lett.* **2006**, *8*, 223−225.
(64) Cox, J. A.; Comte, M.; Fitton, J. E.; DeGrado, W. F. *J. Biol. Chem.* **1985**, *260*, 2527−2534.
(65) Yuan, T.; Vogel, H. J. *Protein Sci.* **1999**, *8*, 113−121.
(66) Crivici, A.; Ikura, M. *Ann. Rev. Biophys. Biomol. Stuct.* **1995**, *24*, 85−116.
(67) Oneil, K. T.; Degrado, W. F. *Trends Biochem. Sci.* **1990**, *15*, 59−64.
(68) Brun, M. P.; Bischoff, L.; Garbay, C. *Angew. Chem., Int. Ed.* **2004**, *43*, 3432−3436.
(69) Bruno, J.; Horrocks, W. D.; Zauhar, R. J. *Biochemistry* **1992**, *31*, 7016−7026.
(70) Gariepy, J.; Sykes, B. D.; Hodges, R. S. *Biochemistry* **1983**, *22*, 1765−1772.
(71) Horrocks, W. D.; Tingey, J. M. *Biochemistry* **1988**, *27*, 413−419.
(72) Ohashi, W.; Hirota, H.; Yamazaki, T. *Protein Sci.* **2011**, *20*, 690−701.
(73) Wu, X. C.; Reid, R. E. *Biochemistry* **1997**, *36*, 8649−8656.
(74) Yang, J. J.; Gawthrop, A.; Ye, Y. Y. *Protein Peptide Lett.* **2003**, *10*, 331−345.
(75) Nitz, M.; Sherawat, M.; Franz, K. J.; Peisach, E.; Allen, K. N.; Imperiali, B. *Angew. Chem., Int. Ed.* **2004**, *43*, 3682−3685.
(76) Banner, D. W.; Bloomer, A. C.; Petsko, G. A.; Phillips, D. C.; Pogson, C. I.; Wilson, I. A.; Corran, P. H.; Furth, A. J.; Milman, J. D.; Offord, R. E.; Priddle, J. D.; Waley, S. G. *Nature* **1975**, *255*, 609−614.
(77) Noble, M. E. M.; Zeelen, J. P.; Wierenga, R. K.; Mainfroid, V.; Goraj, K.; Gohimont, A. C.; Martial, J. A. *Acta Crystallogr. D* **1993**, *49*, 403−417.
(78) Butler, R. S.; Cohn, P.; Tenzel, P.; Abboud, K. A.; Castellano, R. K. *J. Am. Chem. Soc.* **2009**, *131*, 623−633.
(79) Meier, H. *Angew. Chem., Int. Ed.* **2005**, *44*, 2482−2506.
(80) Smith, J. A.; West, R. M.; Allen, M. *J. Fluoresc.* **2004**, *14*, 151−171.
(81) Huang, C.; Yan, S. J.; Li, Y. M.; Huang, R.; Lin, J. *Bioorg. Med. Chem. Lett.* **2010**, *20*, 4665−4669.